Jeffrey D. Stoen
Thomas R. Kane
Department of Mechanical Engineering
Division of Applied Mechanics
Stanford University
Stanford CA 94305

Motion of a Rigid Body Supported at One Point by a Rotating Arm

This article details a scheme for evaluating the stability of motions of a system consisting of a rigid body connected at one point to a rotating arm. The nonlinear equations of motion for the system are formulated, and a method for finding exact solutions representing motions that resemble a state of rest is presented. The equations are then linearized and roots of the eigensystem are classified and used to construct stability diagrams that facilitate the assessment of effects of varying the body's mass properties and system geometry, changing the position of the attachment joint, and adding energy dissipation in the joint. © *1993 John Wiley & Sons, Inc.*

INTRODUCTION

Because it is widely thought that it may be harmful to humans to be in a state of weightlessness for extended periods of time, various schemes for creating an artificial gravity environment for astronauts are currently under investigation. Most of these involve exploitation of the basic fact that underlies the operation of a centrifuge, namely, that each point of a rigid body that is in a state of rotation about an axis fixed both in the body and in an inertial reference frame possesses an acceleration directed toward the axis of rotation. However, because spaceflight structures are required to be relatively light and the dimensions of a rotating space–centrifuge must be large to provide a comfortable living environment, analyses of realistic systems generally involve motions more complicated than those of a single rigid body in a state of simple rotation, such as those performed by two rigid bodies connected by an elastic tether (Robe and Kane, 1967). The analysis that follows deals with an idealized, simplified form of this situation. Specifically, we consider the motion of a rigid body attached by means of a ball-and-socket joint to a rigid arm that is rotating with constant angular speed about an axis fixed in a Newtonian reference frame. Particular attention is focused on effects variously attributable to the placement of the joint relative to the central principal axes of inertia of the body, and to energy dissipation in the joint.

The sequel is arranged as follows. Section 2 contains a brief review of the literature dealing with related problems. In Section 3 the system under consideration is described in detail and differential equations of motion are reported. Exact solutions of these equations are set forth and related stability issues are explored in Section 4.

LITERATURE REVIEW

One of the most important problems in the classical dynamics literature is that of the motion of a single rigid body with one point fixed in inertial space and free of external forces. This problem was first posed by Euler in his *Mémoires de*

Shock and Vibration, Vol. 1, No. 2, pp. 121–134 (1993)

CCC 1070-9622/93/020121-14

Berlin in 1758, and in later years attracted the attention of many talented mathematicians, among them Kirchoff, Poinsott, and Jacobi, the last of whom derived a closed-form solution to the problem in terms of elliptic functions. The problem continues to occupy a central position in satellite attitude dynamics, particularly in regard to simple spin about one of the three central principal axes of inertia of a rigid spacecraft. Investigations of the stability of such motions have led to the well-known "major-axis" rule for spin stabilized satellites (Hughes, 1986), and the single rigid body problem has spawned many elegant analyses that establish a point of departure for the solution of problems closely related to that of a rotating centrifuge.

Studies dealing with stability issues arising in connection with a rotating centrifuge have appeared sporadically in the literature since the late 1960s. In 1967, Robe and Kane (1967) investigated the effects of elastic deformation on the stability of motions of a rotating satellite consisting of two elastically connected, inertially identical, unsymmetrical rigid bodies. They were able to relate instabilities of motions of the deformable vehicle to the instabilities of motions of an associated rigid body, and they demonstrated that the nature of the elastic connection significantly affects the attitude stability of the system. Several years later, Bainum and Evans (1975) analyzed the stability of a rotating cable-connected system consisting of two rigid bodies connected by a massless, extensible tether. They concluded that in-plane stability is insured if either cable damping or rotational damping is present in at least one of the end bodies about an axis nominally perpendicular to the plane of rotation. Furthermore, they demonstrated that out-of-plane stability requires rotational damping on each of the endbodies about at least one of the principal axes that nominally lie in the plane of rotation. Anderson (1969) studied the response of a cable-connected space station to harmonic disturbance torques and concluded that the basic attitude response is that of an undamped second-order system coupled with rigid-body characteristics and cable lateral motion. He also showed that damping due to the viscoelastic bending of the cable does not affect the response of the system appreciably because the tether remains fairly straight and fails to exercise the natural bending induced damping mechanisms. Wilson (1992) used eigenvalue analysis to demonstrate that proper orientation of a cylindrical habitat module provides a stable centrifuge configuration.

What is common to all of the stability studies in the literature to date is that they deal exclusively with cable connections made at the mass center or on central principal axes of the end bodies. In the present work we eliminate these restrictions and pay particular attention to effects of placing the connecting joint at a point that does not lie on central principal axes of inertia. In addition, we attempt to fill the void between the well-understood dynamics of conventional satellites and the dynamics of a space–centrifuge by casting the results of stability predictions for the centrifuge in a form consistent with that of the classical literature, thereby allowing a direct assessment of the unique characteristics of such an arrangement. Following the stability analysis, examples are presented to illustrate the importance of the placement of the cable attachment point and to draw attention to the possibility of destabilization of a nominally stable motion by energy dissipation.

ANALYTICAL MODEL

Although many variations of artificial-gravity spacecraft have been proposed, it is generally agreed that a system consisting of two bodies connected by a long tether probably is the most attractive, considering the lift capacities of current launch vehicles. Although part of the design of such a vehicle will involve trade-off studies to determine the most advantageous sizing of the two bodies, one parameter that is fixed if one intends to match Earth's gravity at a specified constant rotation rate is the distance from the center of mass of the cable-connected system to the crew compartment. Assuming, as we do in the present treatment, that the system has achieved a steady spin rate and is free of external forces, the system mass center will remain fixed in inertial space. With these points in mind, we study the motion of an idealized system that is simple enough to yield manageable equations of motion, but captures the salient features of the behavior of more complicated systems.

The model selected for the present study is shown in Fig. 1, where S is a sleeve supported by a shaft V that is fixed in a Newtonian reference frame N. Rigidly attached to S is an arm A of length L that supports at its end, point Q, a rigid

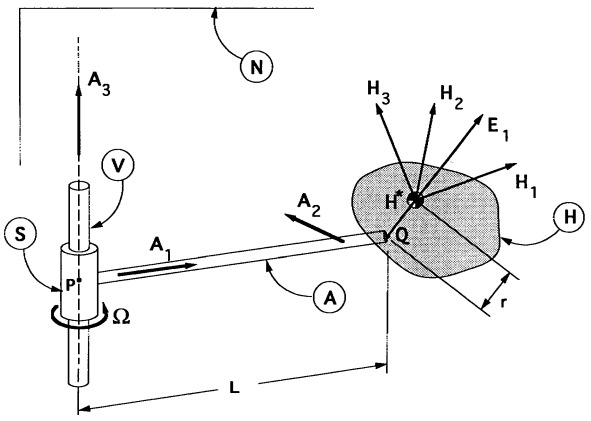

FIGURE 1 Schematic of analytical model.

body H of mass m and unequal central principal moments of inertia I_j ($j = 1, 2, 3$). Friction at the joint located at point Q is accommodated by a torque $\mathbf{T}^{A/H}$ of A on H, with

$$\mathbf{T}^{A/H} = -\sigma\,{}^{A}\omega^{H} \tag{1}$$

where σ is a positive constant and ${}^{A}\omega^{H}$ is the angular velocity of H in A.

In connection with establishing an appropriate set of quantities to define the motion of the system in inertial space we introduce unit vectors $\mathbf{A}_i$ ($i = 1, 2, 3$) fixed in A, with $\mathbf{A}_3$ parallel to the axis of V, and $\mathbf{A}_1$ parallel to the axis of A, as shown in Fig. 1. S is made to rotate in N at a constant angular speed Ω, so that the angular velocity of A in N can be written

$${}^{N}\omega^{A} = \Omega\mathbf{A}_3. \tag{2}$$

To accommodate an off-principal-axes attachment point for H, we introduce a set of mutually perpendicular unit vectors $\mathbf{H}_i$ ($i = 1, 2, 3$) each parallel to a central principal axis of inertia of H, as shown in Fig. 2. Next, we align a set of unit vectors $\mathbf{E}_i$ ($i = 1, 2, 3$) with $\mathbf{H}_i$ ($i = 1, 2, 3$) and subject it first to a dextral rotation of amount θ_1 about $\mathbf{H}_3$, and then to a dextral rotation of amount θ_2 about $-\mathbf{E}_2$ in its current position. An attachment point Q that does not lie on any central principal axis is then readily found by moving from H^* through a distance r in the $-\mathbf{E}_1$ direction (see Fig. 2), and the position vector from H^* to Q is given by

$$\mathbf{p}^{H^*Q} = -r\mathbf{E}_1. \tag{3}$$

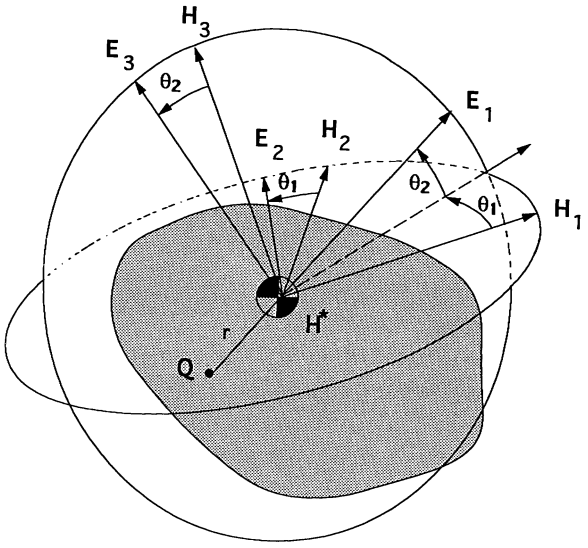

FIGURE 2 Attachment point placement angles θ_1 and θ_2.

The set of unit vectors $\mathbf{E}_i$ ($i = 1, 2, 3$) just constructed and fixed in H is oriented with respect to A by first aligning $\mathbf{E}_i$ ($i = 1, 2, 3$) with $\mathbf{A}_i$ ($i = 1, 2, 3$) and then subjecting the former triad to dextral rotations of amount q_3 about $\mathbf{E}_3$, q_2 about $\mathbf{E}_2$, and q_1 about $\mathbf{E}_1$, as indicated in Fig. 3.

Because the system possesses three degrees of freedom in N, we introduce generalized speeds u_i ($i = 1, 2, 3$), defining these in terms of ${}^{N}\omega^{H}$, the angular velocity of H in N, as

$$u_i \triangleq {}^{N}\omega^{H} \cdot \mathbf{E}_i \ (i = 1, 2, 3). \tag{4}$$

This brings us into position to formulate the equations of motion of H.

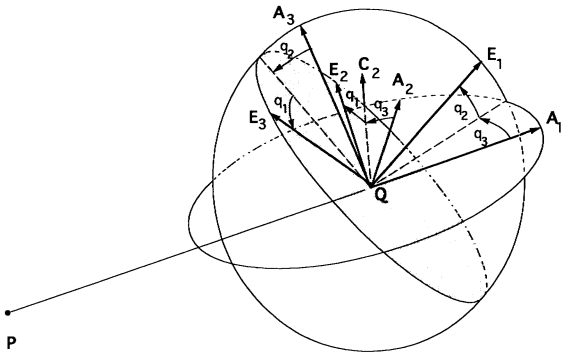

FIGURE 3 Orientation angles q_1, q_2, and q_3.

Equations of Motion

To formulate equations of motion, we begin by introducing the abbreviations

$$s\theta_i \triangleq \sin\theta_i \quad c\theta_i \triangleq \cos\theta_i \quad i = 1, 2 \tag{5}$$

$$sq_i \triangleq \sin q_i \quad cq_i \triangleq \cos q_i \quad i = 1, 2, 3. \tag{6}$$

The kinematical differential equations of motion corresponding to the sequence of rotations performed to orient $\mathbf{E}_i$ ($i = 1, 2, 3$) relative to $\mathbf{A}_i$ ($i = 1, 2, 3$), that is, the equations that relate $\dot{q}_i$ ($i = 1, 2, 3$) to u_i ($i = 1, 2, 3$), are formed as follows.

The angular velocity of H in N is given by

$$^N\omega^H = {}^N\omega^A + {}^A\omega^H \tag{7}$$

where (see Fig. 3 for $\mathbf{C}_2$, definition)

$$^A\omega^H = \dot{q}_3\mathbf{A}_3 - \dot{q}_2\mathbf{C}_2 + \dot{q}_1\mathbf{E}_1. \tag{8}$$

Consequently,

$$^N\omega^H \underset{(2),(7),(8)}{=} \Omega\mathbf{A}_3 + \dot{q}_3\mathbf{A}_3 - \dot{q}_2\mathbf{C}_2 + \dot{q}_1\mathbf{E}_1 \tag{9}$$

(numbers beneath signs of equality refer to corresponding equations). Dot multiplication of this equation with $\mathbf{E}_i$ ($i = 1, 2, 3$) and use of Eq. (4) yields a set of linear equations governing $\dot{q}_i$ ($i = 1, 2, 3$), and the solution of these equations produces the desired kinematical differential equations,

$$\begin{aligned}\dot{q}_1 = u_1 + \tan q_2[&sq_1(\Omega sq_1cq_2 - u_2) \\ &+ cq_1(\Omega cq_1cq_2 - u_3)] - \Omega sq_2\end{aligned} \tag{10}$$

$$\begin{aligned}\dot{q}_2 = &cq_1(\Omega sq_1cq_2 - u_2) \\ &- sq_1(\Omega cq_1cq_2 - u_3)\end{aligned} \tag{11}$$

$$\begin{aligned}\dot{q}_3 = -[&sq_1(\Omega sq_1cq_2 - u_2) \\ &+ cq_1(\Omega cq_1cq_2 - u_3)]/cq_2.\end{aligned} \tag{12}$$

The dynamical differential equations of motion, found with the aid of the symbol manipulation program AUTOLEV (see Appendix), are

$$\begin{aligned}&\dot{u}_1[(I_1 - I_2)s\theta_1^2c\theta_2^2 + (I_1 - I_3)s\theta_2^2 - I_1] + \dot{u}_2(I_1 - I_2)s\theta_1c\theta_1c\theta_2 \\ &+ \dot{u}_3s\theta_2c\theta_2[(I_1 - I_3) - (I_1 - I_2)s\theta_1^2] + (I_1 - I_2)(s\theta_1u_2 - c\theta_1c\theta_2u_1)s\theta_1u_3 \\ &- s\theta_2\{(I_1 - I_3)(s\theta_2u_3 - c\theta_2u_1)u_2 - s\theta_1(I_1 - I_2)[c\theta_1(u_3^2 - u_2^2) \\ &+ s\theta_1u_2(s\theta_2u_3 - c\theta_2u_1)]\} + (I_2 - I_3)u_2u_3 + \sigma[\Omega sq_2 - \dot{q}_1 - \tan q_2(sq_1u_2 \\ &+ cq_1u_3)] = 0\end{aligned} \tag{13}$$

$$\begin{aligned}&\dot{u}_1(I_1 - I_2)s\theta_1c\theta_1c\theta_2 - \dot{u}_2[(I_1 - I_2)s\theta_1^2 + (I_2 + mr^2)] - \dot{u}_3(I_1 - I_2)s\theta_1c\theta_1s\theta_2 \\ &+ s\theta_2(I_1 - I_2)[c\theta_2(u_3^2 - u_1^2) + 2s\theta_2u_1u_3] - (I_1 - I_3 - mr^2)u_1u_3 + s\theta_1(I_1 \\ &- I_2)\{s\theta_1u_1u_3 + c\theta_1c\theta_2u_2u_3 - s\theta_2[s\theta_1c\theta_2(u_3^2 - u_1^2) + 2s\theta_1s\theta_2u_1u_3 \\ &- c\theta_1u_1u_2]\} + Lmr\Omega^2(cq_1sq_2cq_3 - sq_1sq_3) + \sigma[cq_1\dot{q}_2 + sq_1(\Omega cq_2 \\ &- sq_1u_2 - cq_1u_3)] = 0\end{aligned} \tag{14}$$

$$\begin{aligned}&\dot{u}_1s\theta_2c\theta_2[(I_1 - I_3) - (I_1 - I_2)s\theta_1^2] - \dot{u}_2(I_1 - I_2)s\theta_1c\theta_1s\theta_2 + \dot{u}_3[(I_1 \\ &- I_2)s\theta_1^2s\theta_2^2 - (I_1 - I_3)s\theta_2^2 - (I_3 + mr^2)] + (I_1 - I_2 - mr^2)u_1u_2 \\ &- s\theta_2(I_1 - I_3)(s\theta_2u_1u_2 + c\theta_2u_2u_3) + s\theta_1(I_1 - I_2)[c\theta_1c\theta_2u_1^2 - 2s\theta_1u_1u_2 \\ &- c\theta_1c\theta_2u_2^2 - s\theta_2(c\theta_1u_1u_3 - s\theta_1c\theta_2u_2u_3 - s\theta_1s\theta_2u_1u_2)] - Lmr\Omega^2(sq_1sq_2cq_3 \\ &+ cq_1sq_3) + \sigma[\Omega cq_1cq_2 + sq_1(sq_1u_3 - cq_1u_2) - sq_1\dot{q}_2 - u_3] = 0.\end{aligned} \tag{15}$$

STABILITY ANALYSIS

We begin our stability analysis by studying the case of on-axis cable attachment, which leads to a simplified form of Eqs. (10)–(15). Using the results of a linear analysis, we will relate stability predictions to those for a rigid body with one fixed point, thus setting the stage for meaningful interpretation of more general stability results.

On-Axis Attachment, $\theta_1 = \theta_2 = 0$

To place Q on the central principal axis of inertia of H that is parallel to $\mathbf{H}_1$, we set $\theta_1 = \theta_2 = 0$ (see Fig. 2) in Eqs. (10)–(15). In addition, to study motions during which H is permanently at rest in A with $\mathbf{E}_i$ parallel to $\mathbf{A}_i$ ($i = 1, 2, 3$), we set $q_i = \dot{q}_i = 0$ ($i = 1, 2, 3$), $u_1 = u_2 = 0$, $u_3 = \Omega$, and $\dot{u}_i = 0$ ($i = 1, 2, 3$). Under these circumstances, Eqs. (10)–(15) are satisfied identically, which means

that the postulated motion exists. Now we linearize Eqs. (10)–(15) "about this motion" by setting $q_i = \delta q_i$, $\dot{q}_i = \delta\dot{q}_i$ $(i = 1, 2, 3)$, $u_1 = \delta u_1$, $u_2 = \delta u_2$, $u_3 = \Omega + \delta u_3$, and $\dot{u}_i = \delta\dot{u}_i$ $(i = 1, 2, 3)$, and dropping all terms of second or higher degree in δ quantities. Before reporting the resulting linearized equations, we introduce the following parameters:

$$K_1 \triangleq \frac{(I_2 - I_3)}{I_1}, \quad K_2 \triangleq \frac{I_3 + mr^2 - I_1}{I_2 + mr^2}, \tag{16}$$

$$\gamma_2 \triangleq \frac{Lmr}{I_2 + mr^2}, \quad \gamma_3 \triangleq \frac{Lmr}{I_3 + mr^2} \tag{17}$$

$$\sigma_1 \triangleq \frac{\sigma}{I_1}, \quad \sigma_2 \triangleq \frac{\sigma}{I_2 + mr^2}, \quad \sigma_3 \triangleq \frac{\sigma}{I_3 + mr^2}. \tag{18}$$

The linearized equations of motion can now be written

$$\begin{bmatrix} 1 & \sigma_1 & 0 & 0 & 0 & 0 \\ 0 & -1 & 0 & 0 & 0 & 0 \\ 0 & 0 & 1 & -\sigma_2 & 0 & 0 \\ 0 & 0 & 0 & 1 & 0 & 0 \\ 0 & 0 & 0 & 0 & 1 & \sigma_3 \\ 0 & 0 & 0 & 0 & 0 & -1 \end{bmatrix} \begin{Bmatrix} \delta\dot{u}_1 \\ \delta\dot{q}_1 \\ \delta\dot{u}_2 \\ \delta\dot{q}_2 \\ \delta\dot{u}_3 \\ \delta\dot{q}_3 \end{Bmatrix} + \begin{bmatrix} 0 & 0 & -K_1\Omega & 0 & 0 & 0 \\ -1 & 0 & 0 & -\Omega & 0 & 0 \\ -K_2\Omega & 0 & 0 & -\gamma_2\Omega^2 & 0 & 0 \\ 0 & -\Omega & 1 & 0 & 0 & 0 \\ 0 & 0 & 0 & 0 & 0 & \gamma_3\Omega^2 \\ 0 & 0 & 0 & 0 & 1 & 0 \end{bmatrix} \begin{Bmatrix} \delta u_1 \\ \delta q_1 \\ \delta u_2 \\ \delta q_2 \\ \delta u_3 \\ \delta q_3 \end{Bmatrix} = 0. \tag{19}$$

In factored form, the characteristic polynomial for the matrix equation (19) is

$$\begin{aligned} &\{s^2 + \sigma_3 s + \gamma_3\Omega^2\}\{s^4 + (\sigma_1 + \sigma_2)s^3 \\ &\quad + [(1 + \gamma_2 + K_1K_2) + \sigma_1\sigma_2]s^2 \\ &\quad + [-K_1\sigma_2 + (\gamma_2 + K_2)\sigma_1]\Omega^2 s \\ &\quad - K_1(\gamma_2 + K_2)\Omega^4\} = 0. \end{aligned} \tag{20}$$

From Eqs. (19) and (20), we see that the equations governing the quantities δu_3 and δq_3 decouple from the remaining equations. With this in mind, we define as "in-plane" those motions during which all points of H remain equidistant from the plane that passes through Q and is perpendicular to $\mathbf{A}_3$. The decoupling of the in-plane motions from what we shall call out-of-plane motions allows us to characterize the nature of the solutions of Eq. (20) in terms of two physically distinct classes of motion: one associated with the in-plane behavior of the system and described by the quantities δu_3 and δq_3, and one associated with the out-of-plane behavior of the system and described by the quantities δu_1, δq_1, δu_2, and δq_2.

The characteristic roots for the in-plane motion of the system are the zeroes of the quadratic factor in Eq. (20),

$$s_{1,2} = -\frac{\sigma_3}{2} \pm \sqrt{(\sigma_3/2)^2 - \gamma_3\Omega^2}. \tag{21}$$

Both values of s are real if the term inside the radical is positive. This is the case if

$$\sigma^2 > 4Lmr\Omega^2(I_3 + mr^2). \tag{22}$$

If (22) holds, the motion is stable if the inequality

$$\frac{\sigma_3}{2} > \sqrt{(\sigma_3/2)^2 - \gamma_3\Omega^2} \tag{23}$$

is satisfied or, equivalently, if

$$\frac{Lmr}{I_3 + mr^2}\Omega^2 > 0 \tag{24}$$

which is always the case. When (22) is violated, s_1 and s_2 are complex with negative real parts because σ is positive by hypothesis.

The characteristic roots for the out-of-plane equations cannot be expressed in closed form. However, by using the Routh–Hurwitz criteria, we can determine whether or not all roots of the quartic factor in Eq. (20) have negative real parts. All roots of a polynomial of the form

$$s^4 + a_1s^3 + a_2s^2 + a_3s + a_4 = 0 \tag{25}$$

have negative real parts if the following inequalities are satisfied:

$$a_1, a_3, a_4, \Delta_3 > 0 \tag{26}$$

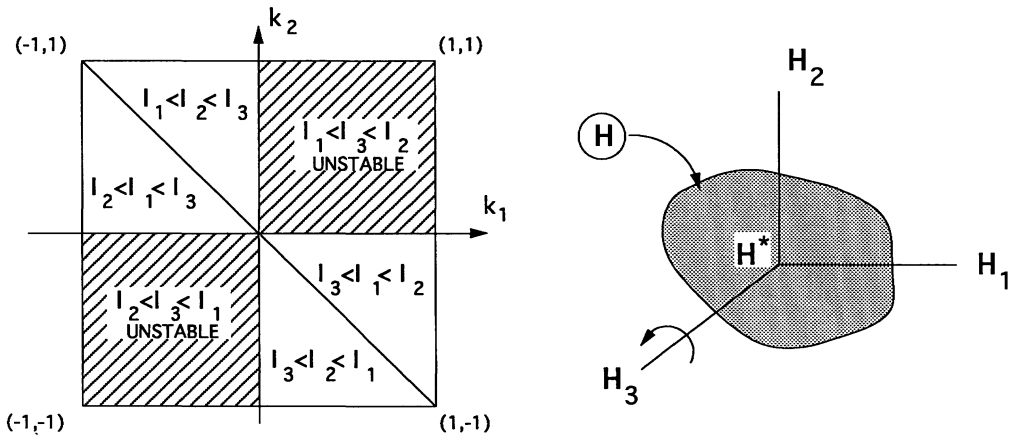

FIGURE 4 Instability chart for a torque-free rigid body with one fixed point.

where

$$\Delta_3 \triangleq det \begin{bmatrix} a_1 & a_3 & 0 \\ 1 & a_2 & a_4 \\ 0 & a_1 & a_3 \end{bmatrix}. \tag{27}$$

Application of these criteria to the quartic factor in Eq. (20) leads to the following

$$(\sigma_1 + \sigma_2) > 0 \tag{28}$$

$$-K_1\sigma_2 + (\gamma_2 + K_2)\sigma_1 > 0 \tag{29}$$

$$-K_1(\gamma_2 + K_2)\Omega^4 > 0 \tag{30}$$

$$(\sigma_1 + \sigma_2)[(1 + \gamma_2 - K_1K_2)\Omega^2 + \sigma_1\sigma_2][-K_1\sigma_2 + (\gamma_2 + K_2)\sigma_1]\Omega^2 + (\sigma_1 + \sigma_2)^2K_1(\gamma_2 + K_2)\Omega^4 - [-K_1\sigma_2 + (\gamma_2 + K_2)\sigma_1)]^2\Omega^4 > 0. \tag{31}$$

Considering the definitions of σ_1 and σ_2 in Eq. (18) and the fact that $\sigma > 0$, we find that (28) is always satisfied. The remaining conditions, (29)–(31), establish relationships between parameters that represent the mass and inertia, geometric, and dissipative properties of the system. Failure to satisfy any of the inequalities (29)–(31) indicates that there are roots of the quartic equation that have positive real parts.

Inequality Interpretation. It is instructive to relate the instabilities of motions of the rigid body supported at one point by a rotating arm to the instabilities of motions of a rigid body with one *fixed* point. The motion of a rigid body whose angular velocity is parallel to a central principal axis, in our case an axis parallel to $\mathbf{B}_3$, is stable if I_3 is the largest or smallest of the three central principal moments of inertia of the body, denoted here by I_1, I_2, and I_3. These facts are commonly discussed in terms of the inertia ratios

$$k_1 = (I_2 - I_3)/I_1, \quad k_2 = (I_3 - I_1)/I_2 \tag{32}$$

where, for any real body,

$$-1 < k_i < 1 \quad (i = 1, 2). \tag{33}$$

Graphically, they may be represented as in Fig. 4.

To establish a relationship between the rigid body inertia ratios (k_1, k_2) and the inertia parameters for our system (K_1, K_2) defined in Eq. (16), an auxiliary parameter ξ is defined as (a similar procedure was used by Robe and Kane, 1967, for flexible vehicles).

$$\xi \triangleq \frac{1}{I_2/mr^2 + 1} \tag{34}$$

where it is noted that

$$0 < \xi < 1. \tag{35}$$

Now, substitution from Eqs. (32) and (34) into Eq. (16) shows that

$$k_1 = K_1 \tag{36}$$

$$k_2 = (K_2 - \xi)/(1 - \xi). \tag{37}$$

We are now in position to contrast motion instability predictions for our system with those rep-

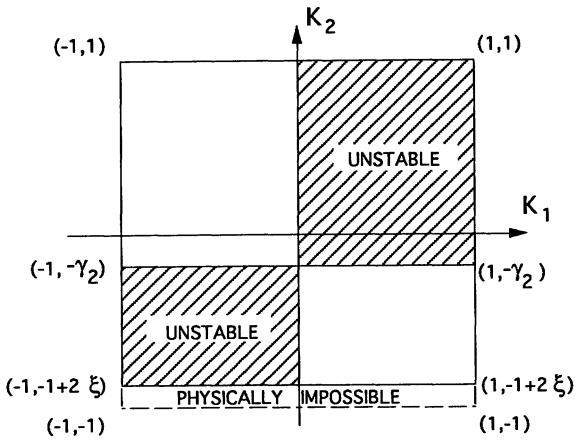

FIGURE 5 First of two instability charts for the system.

resented in Fig. 4 for a rigid body with a fixed point. Beginning with the inequality (30), which is free of damping terms, we see that the Routh–Hurwitz criteria predict negative real parts for all of the quartic roots either if

$$K_1 < 0 \quad \text{and} \quad K_2 > -\gamma_2 \tag{38}$$

or if

$$K_1 > 0 \quad \text{and} \quad K_2 < -\gamma_2. \tag{39}$$

A graphical representation of (38) and (39) is shown in Fig. 5. Figure 5 reduces to Fig. 4 when $\gamma_2 = 0$ and $r = 0$. With reference to Fig. 1, this corresponds to points P, Q, and H^* being all coincident. Figure 5 provides the complete stability picture for the case of zero damping, for which the quartic factor in Eq. (20) reduces to a biquadratic factor. In this event all roots have negative real parts if the single inequality (30) is satisfied. The portion of the figure labeled "PHYSICALLY IMPOSSIBLE" is associated directly with (33), (36), and (37).

It is interesting to note here that for a fully deployed space-centrifuge, $\gamma_2 \gg 1$, which results in instability for all $K_1 > 0$ and stability for all $K_1 \leq 0$. Considering these results in light of Fig. 4, one sees that attachment to a long arm executing simple spin in an inertial frame stabilizes some bodies while it destabilizes others.

Moving to the inequality (29), we now bring into the discussion the effect of adding damping to the system. The inequality may be rearranged to read

$$K_2 > \frac{\sigma_2}{\sigma_1} K_1 - \gamma_2. \tag{40}$$

In a Cartesian plot of K_1 versus K_2, this represents a straight line of slope σ_2/σ_1 and with an intercept $-\gamma_2$ on the K_2 axis. Corresponding to points above this line, all roots of the quartic factor have negative real parts, whereas at least one root has a positive real part if the point (K_1, K_2) lies below the line. These results are presented graphically in Fig. 6. In conjunction with the results of Fig. 5, Fig. 6 shows that damping cannot destabilize the motion of a system with $K_1 < 0$, whereas damping produces an instability in the motion of systems with $K_1 > 0$.

The inequality (31), being quite complex, does not lend itself to simple graphical representation. However, one can use (31) by directly substituting values of the physical parameters of the system into the inequality and determining whether the inequality is satisfied. If it is not, at least one root of the quartic factor in the characteristic Eq. (20) has a positive real part.

Example 1. As already mentioned, the results reported in Figs. 5 and 6 predict that damping can destabilize a nominally stable motion. To demonstrate this, we construct a system with $K_1 = 0.5$ and $K_2 = -0.5$ by proper selection of the physical parameters. Specifically we choose

$$I_1 = 11 \text{ kg m}^2, \quad I_2 = 10 \text{ kg m}^2, \quad I_3 = 4.5 \text{ kg m}^2 \tag{41}$$

$$L = 1 \text{ m}, \quad m = 1 \text{ kg}, \quad r = 1 \text{ m}, \quad \Omega = 1 \text{ rad/s}. \tag{42}$$

Then, using numerical integration of the fully nonlinear equations of motion, Eqs. (10)–(15), we simulate the motion of the system near the "equilibrium" state described by

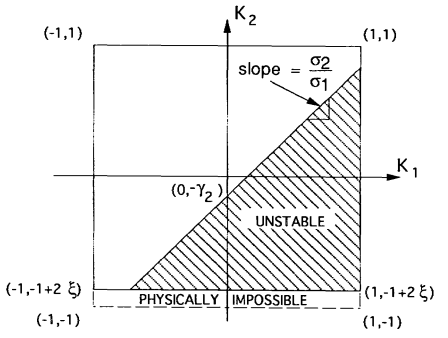

FIGURE 6 Second instability chart for the system.

$$q_i = 0 \quad (i = 1, 2, 3), \quad u_1 = u_2 = 0, \quad u_3 = \Omega. \tag{43}$$

Specifically, we set

$$q_1(0) = q_3(0) = 0°, \quad q_2(0) = 3° \tag{44}$$

$$u_1(0) = \Omega \sin q_2(0), \quad u_2(0) = 0, \quad u_3(0) = \Omega \cos q_2(0). \tag{45}$$

First we consider undamped motions of the system by setting σ equal to zero in Eqs. (10–(15). Results produced by numerical integration for this case are reported in Fig. 7(a,b), where β, the angle between $\mathbf{A}_1$ and $\mathbf{E}_1$, is given by

$$\beta = \cos^{-1}(\cos q_2 \cos q_3). \tag{46}$$

As can be seen from the figures, q_1 and β are consistently bounded with q_1 centered about its equilibrium value of zero. Furthermore, Fig. 7(a,b) clearly demonstrate that a small change in the initial value $\beta(0)$ results in a correspondingly small change in the response of the system.

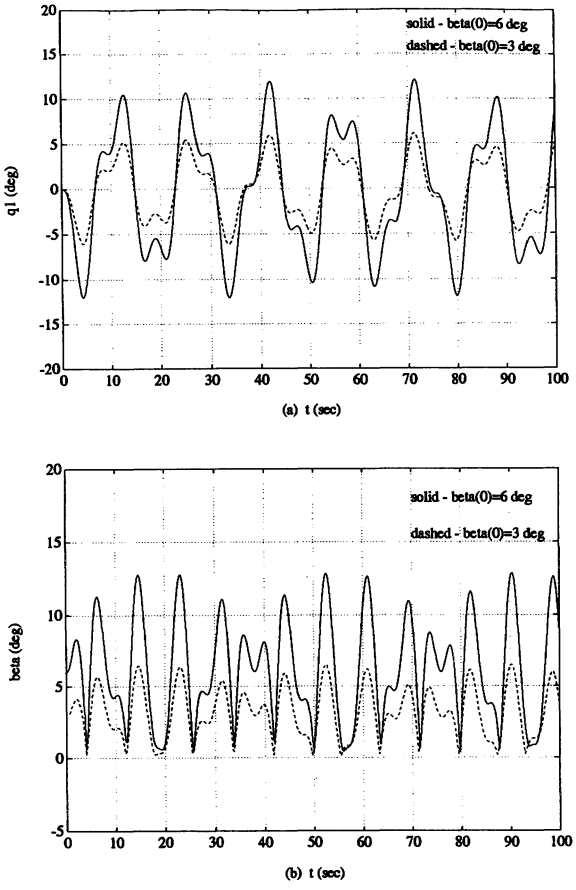

FIGURE 7 Undamped response with on-axis attachment and $K_1 = 0.5$, $K_2 = 0.5$. (a) q_1 (deg), and (b) β (deg).

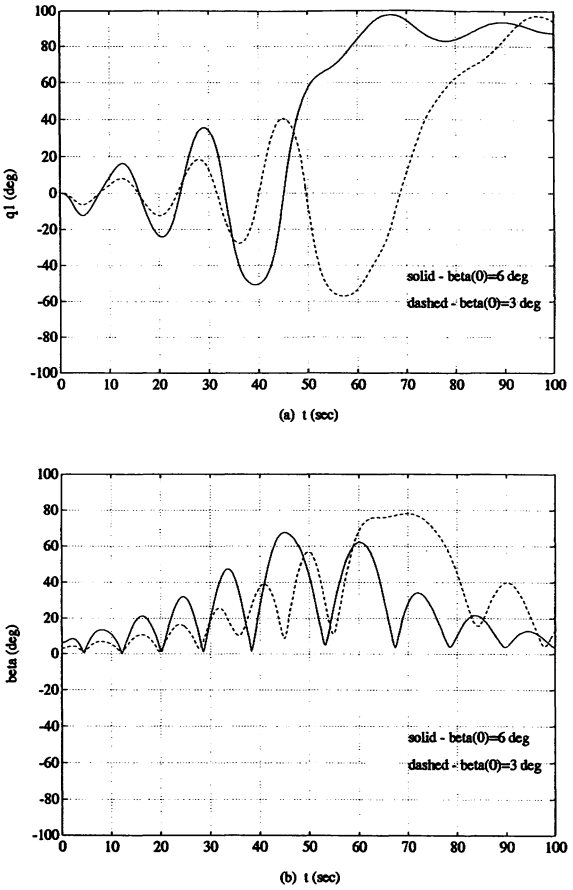

FIGURE 8 Damped response with on-axis attachment and $K_1 = 0.5$, $K_2 = -0.5$. (a) q_1 (deg), and (b) β (deg).

In stark contrast to Fig. 7, Fig. 8(a,b) show the effect of adding damping to the system by setting $\sigma = 1$ N · m · s. As predicted in the stability diagram of Fig. 6, this produces an unstable motion. Even though the exact same initial values are used for the state variables in Figs. 7 and 8, the results of Fig. 8 clearly show the remarkable destabilizing effect of adding damping to the system. In addition, Fig. 8 shows that changing $\beta(0)$ from 3° to 6° has a disproportionately large effect on the response of the system, a classic indication instability.

It is interesting to note that H acquires a new equilibrium position, one such that $q_1 = -90°$. As a result, the axis of minimum moment of inertia, which was originally parallel to $\mathbf{A}_3$, becomes parallel to $\mathbf{A}_2$. This corresponds to $K_1 = -0.5$ and

$K_2 = 0$, which are the coordinates of a point in a region labeled "stable" in Figs. 5 and 6.

Together, Figs. 7(a)–8(b) show that adding energy dissipation at the attachment joint Q can have a destabilizing effect on the response of the system. However, damping does not present a problem for every choice of the parameters K_1 and K_2. By making use of Figs. 5 and 6 together with the inequality (31), one can find system parameters for which the nominal motion is stable both with and without damping. Furthermore, one can select a set of parameters such that the system's response is improved significantly by damping. These facts, as well as a methodology assessing stability in the case of off-axis attachment, are discussed in the next section.

Off-Axis Attachment

In the case of on-principal-axis attachment, we are afforded the luxury of an equilibrium solution such that $q_i = 0$ ($i = 1, 2, 3$). With off-axis attachment, this is no longer the case and a set of nonlinear equations must be solved to find the equilibrium values of the orientation angles q_i ($i = 1, 2, 3$). We can simplify this task by setting the moment about point Q of all inertia forces acting on H equal to zero, which leads to the requirement that q_3 be equal to zero.

Substitution of $q_3 = 0$ along with $\dot{q}_i = 0$ ($i = 1, 2, 3$) into the kinematical differential Eqs. (10)–(12) yields the equilibrium values for u_i ($i = 1, 2, 3$), namely,

$$u_1 = \Omega \sin q_2, \quad u_2 = \Omega \sin q_1 \cos q_2, \quad u_3 = \Omega \cos q_1 \cos q_2. \tag{47}$$

Substituting these values for u_i into the dynamical Eqs. (13)–(15) results in three equations in q_1 and q_2; but it can be shown that satisfaction of any two of the equations guarantees satisfaction of the third because [see Eqs. (49)–(51)]

$$\mathscr{L}_3 = \frac{-sq_2}{cq_1cq_2}\mathscr{L}_1 - \frac{sq_1}{cq_2}\mathscr{L}_2. \tag{48}$$

The equations to be satisfied for equilibrium are

$$\begin{aligned}\mathscr{L}_1 = {} & -\Omega^2 cq_2\langle s\theta_1 cq_1(I_1 - I_2)(c\theta_1 c\theta_2 sq_2 - s\theta_1 sq_1 cq_2) - sq_1 cq_1 cq_2(I_2 - I_3) \\ & - s\theta_2\{sq_1(I_1 - I_3)(c\theta_2 sq_2 - s\theta_2 cq_1 cq_2) - s\theta_1(I_1 - I_2)[c\theta_1 cq_2(-1 \\ & + 2sq_1^2) + s\theta_1 sq_1(c\theta_2 sq_2 - s\theta_2 cq_1 cq_2)]\}\rangle = 0\end{aligned} \tag{49}$$

$$\begin{aligned}\mathscr{L}_2 = {} & -\Omega^2\langle cq_1 sq_2 cq_2(I_1 - I_3 - mr^2) - Lmrcq_1 sq_2 - s\theta_2(I_1 \\ & - I_3)[2s\theta_2 cq_1 sq_2 cq_2 + c\theta_2(cq_1^2 cq_2^2 - sq_2^2)] - s\theta_1(I_1 - I_2)\{s\theta_1 cq_1 sq_2 cq_2 \\ & + c\theta_1 c\theta_2 sq_1 cq_1 cq_2^2 + s\theta_2\{c\theta_1 sq_1 sq_2 cq_2 - 2s\theta_1 s\theta_2 cq_1 sq_2 cq_2 \\ & - s\theta_1 c\theta_2(cq_1^2 cq_2^2 - sq_2^2)]\}\rangle = 0\end{aligned} \tag{50}$$

$$\begin{aligned}\mathscr{L}_3 = {} & \Omega^2\{sq_1 sq_2 cq_2(I_1 - I_2 - mr^2) - Lmrsq_1 sq_2 - s\theta_2 sq_1 cq_2(I_1 \\ & - I_3)(s\theta_2 sq_2 + c\theta_2 cq_1 cq_2) - s\theta_1(I_1 - I_2)[c\theta_1 c\theta_2 sq_1^2 + sq_2(2s\theta_1 sq_1 cq_2 \\ & - c\theta_1 c\theta_2 sq_2 - c\theta_1 c\theta_2 sq_2 sq_1^2) + s\theta_2 cq_2(c\theta_1 cq_1 sq_2 \\ & - s\theta_1 s\theta_2 sq_1 sq_2 - s\theta_1 c\theta_2 sq_1 cq_1 cq_2)]\} = 0.\end{aligned} \tag{51}$$

Any two of these equations can be solved simultaneously by numerical means, such as the Newton–Raphson method. The following example will demonstrate the utility of doing this.

Example 2. Figure 9 depicts a rigid body H supported at point Q by a rotating arm in the same fashion as depicted in Fig. 1 except that now Q can be made to move relative to H by a two-axis actuator that is capable of positioning Q at any point (x, y) within a 1×1 m square normal to $\mathbf{H}_1$. (A scheme for stabilizing the motions of a space-centrifuge using a movable attachment point has been proposed by Thornburg and Powell, 1993). The system parameters are

$$I_1 = 165{,}000 \text{ kg m}^2, \quad I_2 = 53{,}000 \text{ kg m}^2, \quad I_3 = 165{,}000 \text{ kg m}^2 \tag{52}$$

$$L = 224 \text{ m}, \quad m = 20{,}000 \text{ kg}, \quad d = 4.6 \text{ m}, \quad \Omega = 0.21 \text{ rad/s}. \tag{53}$$

If the system is initially configured with $(x, y) = (0, 0)$, which means that Q lies on a line parallel to $\mathbf{H}_1$, we know that the equilibrium values of the orientation angles are $q_i = 0$ ($i = 1, 2$). If Q is now moved to the extreme ends of travel, so that $x = y = 0.5$ m, a new equilibrium solution for q_i ($i = 1, 2$) results. We may find it as follows.

The attachment point placement angles θ_1 and θ_2 defined in Fig. 2, expressed in terms of x and y, are given by

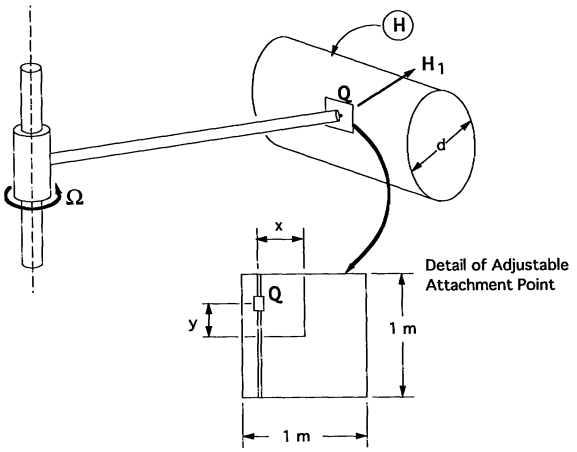

FIGURE 9 Example system with adjustable, off-axis attachment.

$$\theta_1 = \tan^{-1}\left(\frac{x}{d/2}\right) = \tan^{-1}\left(\frac{0.5}{2.3}\right) = 12.3° \quad (54)$$

$$\theta_2 = \tan^{-1}\left(\frac{y}{\sqrt{(d/2)^2 + x^2}}\right) = \tan^{-1}\left(\frac{0.5}{\sqrt{(2.3)^2 + 0.5^2}}\right) = 12.0°. \quad (55)$$

Substituting these values of θ_1 and θ_2 into Eqs. (49) and (50) along with the numerical values of the system parameters from Eqs. (52) and (53), and solving the resulting set of equations numerically, we obtain the equilibrium values

$$q_1 = 2.6°, \quad q_2 = 0°. \quad (56)$$

Linearization. Denoting the equilibrium values of q_1 and q_2 that satisfy Eqs. (49)–(51) as $\bar{q}_1$ and $\bar{q}_2$, we linearize Eqs. (10)–(15) about this equilibrium solution and report the results as the matrix equation

$$\begin{bmatrix} A_{11} & A_{12} & A_{13} & 0 & A_{15} & 0 \\ 0 & -1 & 0 & 0 & 0 & -s\bar{q}_2 \\ A_{31} & 0 & A_{33} & A_{34} & A_{35} & 0 \\ 0 & 0 & 0 & c\bar{q}_1 & 0 & -s\bar{q}_1 c\bar{q}_2 \\ A_{51} & 0 & A_{53} & A_{54} & A_{55} & 0 \\ 0 & 0 & 0 & s\bar{q}_1 & 0 & -c\bar{q}_1 c\bar{q}_2 \end{bmatrix} \begin{Bmatrix} \delta\dot{u} \\ \delta\dot{q}_1 \\ \delta\dot{u}_2 \\ \delta\dot{q}_2 \\ \delta\dot{u}_3 \\ \delta\dot{q}_3 \end{Bmatrix} + \begin{bmatrix} B_{11} & 0 & B_{13} & B_{14} & B_{15} & 0 \\ 1 & 0 & 0 & -\Omega c\bar{q}_2 & 0 & 0 \\ B_{31} & B_{32} & B_{33} & B_{34} & B_{35} & B_{36} \\ 0 & -\Omega c\bar{q}_1 c\bar{q}_2 & 1 & \Omega s\bar{q}_1 s\bar{q}_2 & 0 & 0 \\ B_{51} & B_{52} & B_{53} & B_{54} & B_{55} & B_{56} \\ 0 & \Omega s\bar{q}_1 c\bar{q}_2 & 0 & \Omega s\bar{q}_2 c\bar{q}_1 & 1 & 0 \end{bmatrix} \begin{Bmatrix} \delta u_1 \\ \delta q_1 \\ \delta u_2 \\ \delta q_2 \\ \delta u_3 \\ \delta q_3 \end{Bmatrix} = 0 \quad (57)$$

where A_{ij} and B_{ij} are defined as

$$A_{11} \triangleq s\theta_2^2(I_1 - I_3) + c\theta_2^2 s\theta_1^2(I_1 - I_2) - I_1; \qquad A_{12} \triangleq -\sigma$$
$$A_{13} \triangleq s\theta c\theta_1 c\theta_2(I_1 - I_2)$$
$$A_{15} \triangleq s\theta_2 c\theta_2[I_1 - I_3 - s\theta_1^2(I_1 - I_2)]$$
$$A_{31} \triangleq s\theta_1 c\theta_1 c\theta_2(I_1 - I_2)$$
$$A_{33} \triangleq -I_2 - mr^2 - s\theta_1^2(I_1 - I_2); \qquad A_{34} \triangleq \sigma c\bar{q}_1$$
$$A_{35} \triangleq -c\theta_1 s\theta_1 s\theta_2(I_1 - I_2)$$

$$A_{51} \triangleq s\theta_2 c\theta_2[I_1 - I_3 - s\theta_1^2(I_1 - I_2)]$$

$$A_{53} \triangleq -s\theta_1 c\theta_1 s\theta_2(I_1 - I_2); \qquad A_{54} \triangleq -\sigma s\bar{q}_1$$

$$A_{55} \triangleq s\theta_1^2 s\theta_2^2(I_1 - I_2) - I_3 - mr^2 - s\theta_2^2(I_1 - I_3)$$

$$B_{11} \triangleq -\Omega c\theta_2 c\bar{q}_2\{s\theta_1 c\theta_1 c\bar{q}_1(I_1 - I_2) - s\theta_2 s\bar{q}_1[I_1 - I_3 - s\theta_1^2(I_1 - I_2)]\}$$

$$B_{13} \triangleq \Omega c\bar{q}_1 c\bar{q}_2(I_2 - I_3) + \Omega s\theta_1^2 c\bar{q}_1 c\bar{q}_2(I_1 - I_2) + \Omega s\theta_2\{(I_1 - I_3)(c\theta_2 s\bar{q}_2 - s\theta_2 c\bar{q}_1 c\bar{q}_2) - s\theta_1(I_1 - I_2)[2c\theta_1 s\bar{q}_1 c\bar{q}_2 + s\theta_1(c\theta_2 s\bar{q}_2 - s\theta_2 c\bar{q}_1 c\bar{q}_2)]\} - \sigma s\bar{q}_1 \tan(\bar{q}_2)$$

$$B_{14} \triangleq -\sigma\Omega \tan(\bar{q}_2) s\bar{q}_2$$

$$B_{15} \triangleq \Omega s\bar{q}_1 c\bar{q}_2(I_2 - I_3) - \sigma c\bar{q}_1 \tan(\bar{q}_2) - \Omega s\theta_1(I_1 - I_2)(c\theta_1 c\theta_2 s\bar{q}_2 - \bar{s}\theta_1 s\bar{q}_1 c\bar{q}_2) - \Omega s\theta_2 c\bar{q}_2[s\theta_2 s\bar{q}_1(I_1 - I_3) - s\theta_1(I_1 - I_2)(2c\theta_1 c\bar{q}_1 + s\theta_1 s\theta_2 s\bar{q}_1)]$$

$$B_{31} \triangleq -\Omega\{c\bar{q}_1 c\bar{q}_2(I_1 - I_3 - mr^2) + 2s\theta_2(I_1 - I_3)(c\theta_2 s\bar{q}_2 - s\theta_2 c\bar{q}_1 c\bar{q}_2) - s\theta_1(I_1 - I_2)[s\theta_1 c\bar{q}_1 c\bar{q}_2 + s\theta_2(2c\theta_2 s\theta_1 s\bar{q}_2 + c\theta_1 s\bar{q}_1 c\bar{q}_2 - 2s\theta_1 s\theta_2 c\bar{q}_1 c\bar{q}_2)]\}$$

$$B_{32} \triangleq -Lmr\Omega^2 s\bar{q}_1 s\bar{q}_2$$

$$B_{33} \triangleq \Omega s\theta_1 c\theta_1(I_1 - I_2)(s\theta_2 s\bar{q}_2 + c\theta_2 c\bar{q}_1 c\bar{q}_2) - \sigma s\bar{q}_1^2 \qquad (58)$$

$$B_{34} \triangleq -\Omega(\sigma s\bar{q}_1 s\bar{q}_2 - Lmr\Omega c\bar{q}_1 c\bar{q}_2)$$

$$B_{35} \triangleq 2\Omega s\theta_2(I_1 - I_3)(s\theta_2 s\bar{q}_2 + c\theta_2 c\bar{q}_1 c\bar{q}_2) + \Omega s\theta_1(I_1 - I_2)[s\theta_1 s\bar{q}_2 + c\theta_1 c\theta_2 s\bar{q}_1 c\bar{q}_2 - 2s\theta_1 s\theta_2(s\theta_2 s\bar{q}_2 + c\theta_2 c\bar{q}_1 c\bar{q}_2)] - \sigma s\bar{q}_1 c\bar{q}_1 - \Omega s\bar{q}_2(I_1 - I_3 - mr^2)$$

$$B_{36} \triangleq -Lmr\Omega^2 s\bar{q}_1$$

$$B_{51} \triangleq -\Omega\{s\theta_2^2 s\bar{q}_1 c\bar{q}_2(I_1 - I_3) - s\bar{q}_1 c\bar{q}_2(I_1 - I_2 - mr^2) - s\theta_1(I_1 - I_2)[2c\theta_1 c\theta_2 s\bar{q}_2 - 2s\theta_1 s\bar{q}_1 c\bar{q}_2 - s\theta_2 c\bar{q}_2(c\theta_1 c\bar{q}_1 - s\theta_1 s\theta_2 s\bar{q}_1)]\}$$

$$B_{52} \triangleq -Lmr\Omega^2 c\bar{q}_1 s\bar{q}_2$$

$$B_{53} \triangleq \Omega s\bar{q}_2(I_1 - I_2 - mr^2) - \sigma s\bar{q}_1 c\bar{q}_1 - \Omega s\theta_2(I_1 - I_3)(s\theta_2 s\bar{q}_2 + c\theta_2 c\bar{q}_1 c\bar{q}_2) - \Omega s\theta_1(I_1 - I_2)[2s\theta_1 s\bar{q}_2 + 2c\theta_1 c\theta_2 s\bar{q}_1 c\bar{q}_2 - s\theta_1 s\theta_2(s\theta_2 s\bar{q}_2 + c\theta_2 c\bar{q}_1 c\bar{q}_2)]$$

$$B_{54} \triangleq -\Omega(\sigma c\bar{q}_1 s\bar{q}_2 + Lmr\Omega s\bar{q}_1 c\bar{q}_2)$$

$$B_{55} \triangleq -\sigma c\bar{q}_1^2 - \Omega s\theta_2 c\theta_2 s\bar{q}_1 c\bar{q}_2(I_1 - I_3) - \Omega s\theta_1 s\theta_2(I_1 - I_2)(c\theta_1 s\bar{q}_2 - s\theta_1 c\theta_2 s\bar{q}_1 c\bar{q}_2)$$

$$B_{56} \triangleq -Lmr\Omega^2 c\bar{q}_1.$$

Because Eq. (57) represents a set of linear, ordinary differential equations with constant coefficients, we may study the stability of their null by examining the roots of the associated characteristic equation. To this end, we evaluate the characteristic roots with MATLAB (Moler, Little, Bangert, and Kleiman, 1985) and construct a stability diagram by varying the quantities K_1 and K_2 and examining each of six characteristic roots at evenly spaced intervals. If *any* one of the roots has a positive real part, an "o" is marked on the $K_1 - K_2$ plot. If all of the roots have negative real parts, a "+" is plotted. Additionally, we can study the effects of moving Q off the principal axis aligned with $\mathbf{H}_1$ for a specific system. In this case, K_1 and K_2 and the remaining system parameters are fixed and we vary the attachment offset angles θ_1 and θ_2. Then, by using "o" and "+" as described above, we may chart the effects of varying these angles in a plot of θ_1 versus θ_2. The following illustrative example demonstrates these points.

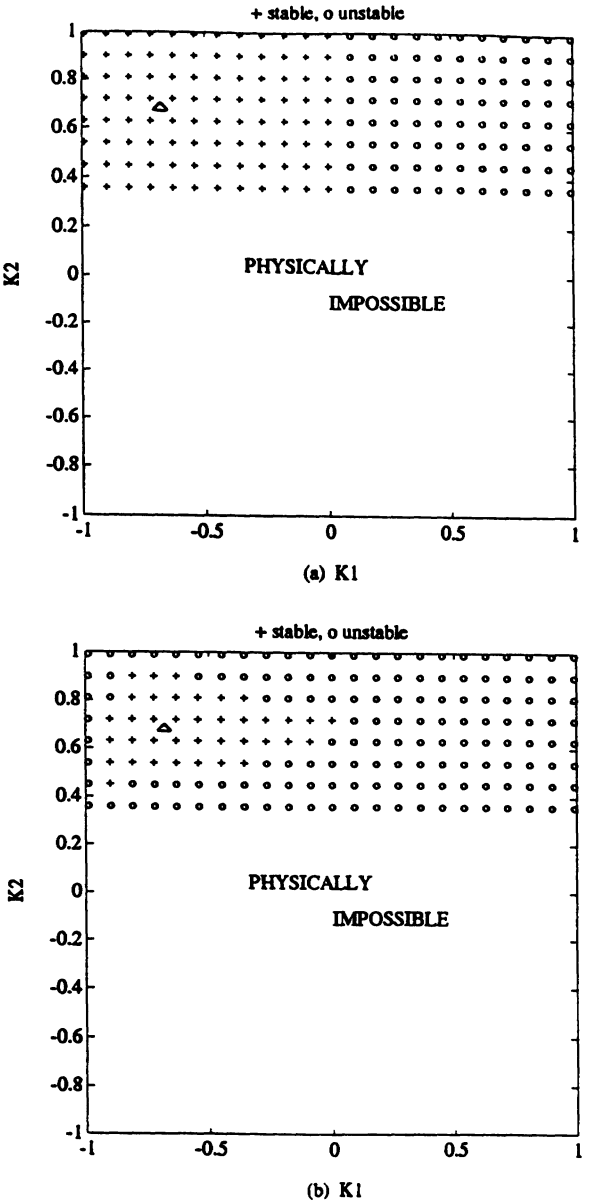

FIGURE 10 Stability diagrams for Example 3, (a) $\theta_1 = \theta_2 = 0°$, (b) $\theta_1 = 12.3°$, $\theta_2 = 12.0°$.

Example 3. In the previous example we found that an off-axis shift in Q is accompanied by a shift in the null solution of Eqs. (49)–(51). Using the methods described above we now are able to construct a stability diagram for the system described in Example 2 and to study the effects of moving the attachment point off the principal axes. Figure 10(a) shows a stability diagram constructed in this way by varying K_1 and K_2 while leaving m and L fixed and equal to the values reported in Eq. (53), and with $r = 2.4$ m. For this figure, we set the offset angles θ_1 and θ_2 equal to zero. The inertia values of Eq. (52), when substituted into Eq. (16), define a point marked with a triangle "Δ" in Fig. 10(a) that is located in a region of the figure that is stable, as denoted by "+". Figure 10(b) shows the effect of setting $\theta_1 = 12.3°$ and $\theta_2 = 12.0°$. As is obvious from the figure, parts of the stable region in the diagram have changed to unstable, an indication that at least one root of the characteristic equation has acquired a positive real part by moving Q off-axis. Fortunately the system we have chosen remains stable with this change, as evidenced by the location of the triangle in Fig. 10(b), as well as by the system response plotted in Fig. 11. The figure shows that the response is a smoothly damped harmonic centered about the equilibrium value of $\bar{q}_1 = 2.6°$. Two plots are included to demonstrate that small changes in the initial value of $q_1(0)$ results in correspondingly small changes in the system's response.

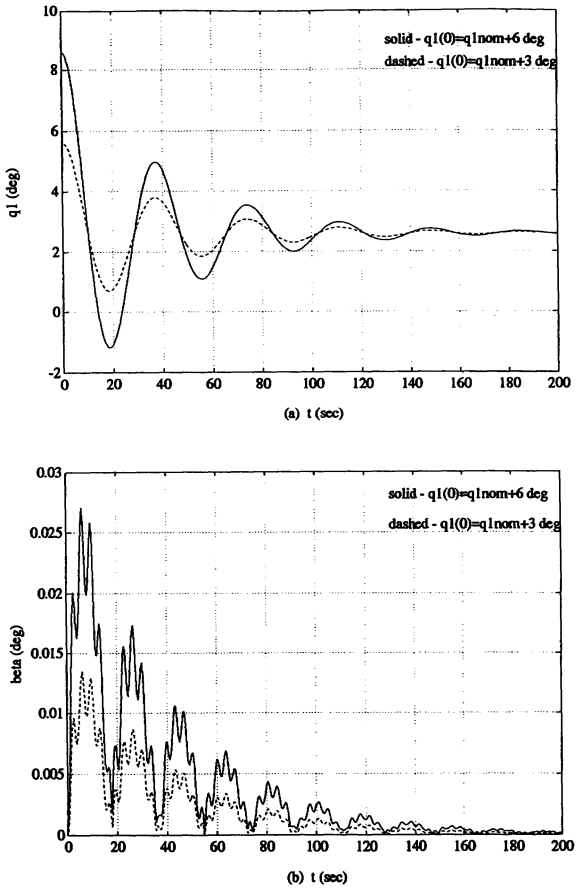

FIGURE 11 Simulation results for a system with off-axis attachment. (a) q_1 (deg), and (b) β (deg).

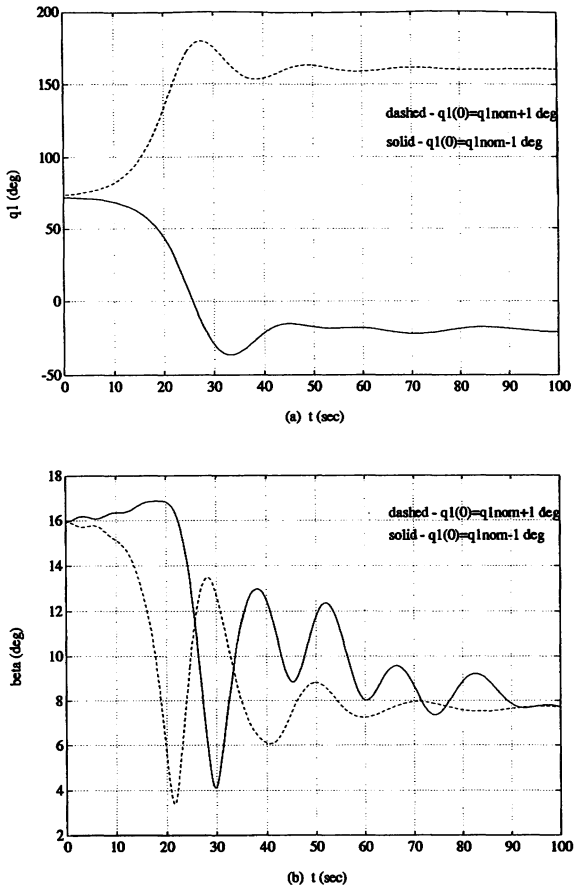

FIGURE 12 Unstable response of a system with off-axis attachment. (a) q_1 (deg), and (b) β (deg).

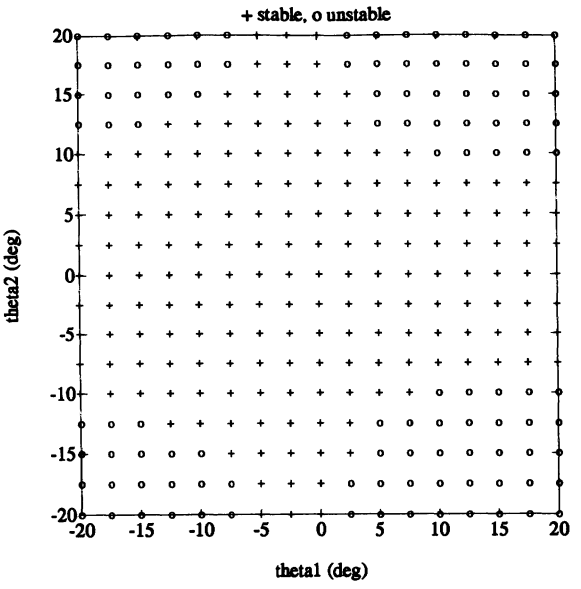

FIGURE 13 Stability diagram demonstrating sensitivity to off-axis attachment.

To demonstrate a case that is more susceptible to developing problems with an off-axis attachment we consider the response of a system with

$$I_1 = 2.3 \text{ kg m}^2, \quad I_2 = 10 \text{ kg m}^2, \quad I_3 = 10.2 \text{ kg m}^2 \tag{59}$$

$$L = 0.5 \text{ m}, \quad m = 1 \text{ kg}, \quad r = 1 \text{ m}, \quad \Omega = 1 \text{ rad/s}. \tag{60}$$

The attachment point placement angles are taken to be $\theta_1 = \theta_2 = 15°$. Numerical solution of Eqs. (49) and (50) yields, as one of several equilibrium solutions,

$$q_1 = 74.2°, \quad q_2 = 16.0°. \tag{61}$$

The results of numerical integration of Eqs. (10)–(15) near this equilibrium are reported in Figs. 12(a,b). We use as initial values

$$q_1(0) = 74.2° \pm 1°, \quad q_2(0) = 16.0°, \quad q_3(0) = 0° \tag{62}$$

$$u_1(0) = \Omega \sin q_2(0), \quad u_2(0) = \Omega \sin q_1(0) \cos q_2(0) \tag{63}$$

$$u_3(0) = \Omega \cos q_1(0) \cos q_2(0). \tag{64}$$

The figures show that changing $q_1(0)$ from one degree above to one degree below the equilibrium value results in markedly different responses for both q_1 and β. The system acquires new q_1 and β equilibria that are far removed from those of Eq. (61). It should also be noted that a slight change in the initial value $q_1(0)$ results in a completely different final value for q_1. Construction of a stability diagram by varying θ_1 and θ_2 from $-20°$ to $20°$, as shown in Fig. 13, clearly demonstrates the sensitivity of this arrangement to accurate on-axis attachment.

APPENDIX

A AUTOLEV Input

```
% End_off2:
%
% Generalized Coordinates
%          Q1: Body Yaw angle.
%          Q2: Body Roll angle.
%          Q3: Body Pitch angle.
%
AUTOZ     ON      % Program can introduce it's own Zees.
VARIABLES     U[3],W      % Number of generalized speeds.
%
% Variables, constants, specified, and actions.
VARIABLES     Q[3]
CONSTANTS     L, R, THETA1, THETA2, OMEGA
```

```
UNITS      THETA1,DEG,THETA2,DEG,Q1,DEG,Q2,DEG,Q3,DEG
UNITS      OMEGA,RAD/SEC
%
% Bodies, frames, points, and particles.
NEWTONIAN      N
FRAMES      A,C,D,E,G
BODIES      H
POINTS      Q,O
%
% Masses of bodies and particles, Inertia of bodies.
MASS      H, M
INERTIA      H,I1,I2,I3
%
% Geometry relating unit vectors (SIMPROT, BODY123, EULER...).
W_A_N> = OMEGA*A3>
SIMPROT(N, A, 3, OMEGA*T)
SIMPROT(B, C, 3, Q3)
SIMPROT(C, D, -2, Q2)
SIMPROT(D, E, 1, Q1)
SIMPROT(E, G, 2, THETA2)
SIMPROT(G, H, -3, THETA1)
%
% Kinematical differential equations.
W_E_A> = Q3'*A3> - Q2'*C2> + Q1'*D1>
WEN> = W_E_A> + W_A_N>
W_E_N> = U1*E1> + U2*E2> + U3*E3>
TEMP> = WEN>-W_E_N>
ZERO[1]=DOT(TEMP>,E1>)
ZERO[2]=DOT(TEMP>,E2>)
ZERO[3]=DOT(TEMP>,E3>)
SOLVE(ZERO,Q1',Q2',Q3')
%
% Angular velocities.
W_H_N> = W_E_N>
%
% Position vectors.
P_O_Q> = L*A1>
P_Q_HSTAR> = R*E1>
%
% Velocities of relevant points.
V_O_N> = 0>
V2PTS(N, A, O, Q)
V2PTS(N, E, Q, HSTAR)
%
% Applied forces and torques of applied couples.
CONSTANTS      K
TORQUE(A/E,-K*W_E_A>)
%
% Form equations of motion.
ZERO = FR() + FRSTAR()
%
% Solve for constraint forces. Put equations into proper form.
KANE()
%
% Forming Kinetic Energy.
KE0 = KE0()
KE2 = KE2()
%
% Forming Activity.
G = FR()
VHSTARNT> = REM(U, V_HSTAR_N>)
DVT> = DT(VHSTARNT>, N)
VDOTDVT = DOT(V_HSTAR_N>, DVT>)
WHNT> = REM(U, W_H_N>)
DWT> = DT(WHNT>, N)
IDOTDWT> = DOT(I_H_HSTAR>>, DWT>)
WDOTIDOTDWT = DOT(W_H_N>, IDOTDWT>)
SIG = M*RHS(VDOTDVT) + RHS(WDOTIDOTDWT)
W' = -G[1]*U1-G[2]*U2-G[3]*U3+RHS(SIG)
%
% Forming Checking Function.
PE = 0
CHECK = RHS(PE) + W + RHS(KE2) - RHS(KE0)
%
% Create simulation code.
RESULTS      T,U1,U2,U3,Q1,Q2
RESULTS      T,Q3,CHECK,W,KE2,KE0
RESULTS      T,HN1,HN2
CODE      END_OFF2
```

REFERENCES

Anderson, W. W., 1969, *On Lateral Cable Oscillations of Cable-Connected Space Stations*. NASA TN 5107, Langley Research Center, Hampton, VA.

Bainum, P. M., and Evans, K. S., 1975, *Three-Dimensional Motion and Stability of Two Rotating Cable-Connected Bodies, Journal of Spacecraft and Rockets,* 1975, Vol. 12, pp. 242–250.

Hughes, P. C., 1986, *Spacecraft Attitude Dynamics,* John Wiley & Sons, Inc., Toronto, Canada, pp. 140–146.

Moler, C., Little, J., Bangert, S., and Kleiman, S., 1985, *MATLAB User's Manual,* The MathWorks, Inc., pp. 242–250.

Robe, T. R., and Kane, T. R., 1967, "Dynamics of an Elastic Satellite—I, II, III," *International Journal of Solids and Structures,* Vol. 3, pp. 333–352, 691–703, 1031–1051.

Thornburg, S. L., and Powell, J. D., *Thrusterless Vibration Control for Tethered Artificial Gravity Spacecraft,* Proceedings of the AAS/AIAA Astrodynamics Specialist Conference, Victoria, B.C., August 16–19, 1993, paper no. AAS-93-734.

Wilson, J. M., 1992, "Control of a Tethered Artificial Gravity Spacecraft," PhD Thesis, Stanford University, pp. 30–38.